Chinese Chemical Letters 37 (2026) 112140

Contents lists available at ScienceDirect

Chinese Chemical Letters

journal homepage: www.elsevier.com/locate/cclet

Discovery a plasiatine-based potent SHP2 activator as a potential anti-atherosclerotic agent

Xuyang Ding, Tongtong Geng, Yongxia Li, Pengming Pan, Zhongtang Li, Zhongjun Li*, Xiangbao Meng*

State Key Laboratory of Natural and Biomimetic Drugs, Department of Chemical Biology, School of Pharmaceutical Sciences, Peking University, Beijing 100191, China

ARTICLE INFO

Article history:
Received 27 July 2025
Revised 19 November 2025
Accepted 20 November 2025
Available online 21 November 2025

Keywords:
SHP2 activator
Plasiatine
Total synthesis
Structure-activity relationship
Anti-atherosclerosis

ABSTRACT

The Src homology 2 domain-containing phosphatase 2 (SHP2) plays a pivotal role in cellular processes and is associated with various diseases. Activation of SHP2 has been shown to be effective in inflammation-related diseases such as colitis, atherosclerosis and Parkinson's disease. Although SHP2 inhibitors have been extensively studied in recent years, especially allosteric inhibitors, only a small number of SHP2 activators exhibiting weak activation effects have been reported. Herein, we developed a facile approach to the total synthesis of plasiatine, which was extracted from the seeds of Plantago asiatica as a direct SHP2 activator. Iterative study on the structure-activity relationship identified a potent SHP2 activator, compound **C8**, with median effective concentration (EC_{50}) = 0.11 μmol/L and E_{max} = 3.75-fold. Surface plasmon resonance experiment revealed a robust binding affinity between **C8** and the SHP2 catalytic domain, with a dissociation constant (K_d) of 70.4 nmol/L. *In vivo* study showed that **C8** significantly reduced atherosclerotic plaques and increased anti-inflammatory factors, highlighting its potential as an effective anti-atherosclerotic agent.

© 2026 Published by Elsevier B.V. on behalf of Chinese Chemical Society and Institute of Materia Medica, Chinese Academy of Medical Sciences.

Src homology 2 domain-containing phosphatase 2 (SHP2) encoded by protein tyrosine phosphatase non-receptor type 11 (PTPN11) gene is a 68 kDa protein tyrosine phosphatase (PTP) containing two Src homologous structure domains (SH2), a conserved catalytic domain and a flexible C-terminal tail with two phosphorylation sites [1]. SHP2 has a context-dependent dual role in cancer, acting as both a promoter and a suppressor [2,3]. SHP2 is associated with a large number of tumor cell signaling pathways, regulating rat sarcoma virus oncogene homolog-extracellular signal-regulated kinase (RAS-ERK) [4], phosphatidylinositol 3-kinase-protein kinase B (PI3K-AKT) [5,6], and Janus Kinase-Signal Transducer and Activator of Transcription (JAK-STAT) [7] signaling pathways and serves as a key mediator of immune checkpoint pathway mediating immune evasion of tumor cells [8–10]. However, SHP2 can also play a cancer suppressing role in glioma, myeloma [11], and colon cancer [12].

In addition, recent evidences are mounting that SHP2 plays an important role in the regulation of inflammation related diseases [13,14]. SHP2 inhibits the sustained activation of STAT3 in DU145 cells and inhibits the inflammatory response [15]. SHP2 inhibits inflammation by disrupting the interaction between STAT3 and interleukin-6 receptor alpha (IL-6Rα) and inhibits the activation of STAT3 to block Th17 differentiation, and effectively relieves colitis in mice [16]. Activation of SHP2 effectively enhances Parkin-mediated mitochondrial autophagy, and significantly reduces neuroinflammation in Parkinson mice [17].

SHP2 activators can be divided into direct activators and indirect activators according to their binding properties. Direct activators include CG902 [15], plasiatine [18], oleanolic acid [16,19], lovastatin [17] and ethacrynic acid [20]. Indirect activators include trichomide A [21] and fusaruside [22] . Most of them are natural products or clinically used drugs and exhibit weak activation effects (Fig. S1 in Supporting information).

Atherosclerosis, a chronic inflammatory disease driven by lipids [23], involves macrophages that take up oxidized low-density lipoproteins (ox-LDL) [24] and release pro-inflammatory factors [25], leading to foam cell formation and plaque accumulation [26,27]. The effectiveness of various anti-inflammatory therapies for atherosclerosis has been extensively investigated [28–31]. Very recently, Ke *et al.* demonstrated that SHP2 promoted anti-inflammatory polarization and efferocytosis in macrophages by stabilizing peroxisome proliferator-activated receptor γ (PPARγ) [32]. Therefore, developing anti-inflammatory drugs based on SHP2 acti-

* Corresponding authors.
E-mail addresses: zjli@bjmu.edu.cn (Z. Li), xbmeng@bjmu.edu.cn (X. Meng).

https://doi.org/10.1016/j.cclet.2025.112140
1001-8417/© 2026 Published by Elsevier B.V. on behalf of Chinese Chemical Society and Institute of Materia Medica, Chinese Academy of Medical Sciences.

vator is expected to become an effective anti-atherosclerosis strategy.

Plasiatine, extracted from the seeds of *Plantago asiatica*, attracted our attention due to its relatively high phosphatase activation activity, which enhanced the SHP2 activity with median effective concentration (EC_{50}) = 0.97 μmol/L [18]. However, plasiatine contains three chiral centers with a novel scaffold assembled with an indole alkaloid and a phenylpropanol moiety *via* the dihydrofuran core. Due to the complexity of its structure, there is no total synthesis work achieved so far. Herein, we report the first total synthesis of plasiatine and the structure-activity relationship of a series of novel plasiatine analogues. Compound **C8** was shown to be a potent SHP2 activator and an effective anti-atherosclerotic agent.

Our research began with total synthesis of plasiatine and its isomers. Given that plasiatine containing three chiral centers assembled indole alkaloid and phenylpropanol together *via* the dihydrofuran core, construction of this new scaffold by cyclization reaction is crucial. Particularly, the configuration of the chiral center needs to be considered meticulously. However, there was no relevant studies towards the construction of this new scaffold, and some relevant chiral synthesis provided poor selectivity [33,34]. Our proposed synthetic routes to plasiatine are shown in Scheme S1 (Supporting information). Route 1 involves the preparation of **S1** and **S2** from 5-methoxyisatin and *trans*-ferulic acid, respectively, followed by cyclization to obtain **S3**, which is expected to be further transformed into plasiatine. In Route 2, we envisage that **S4** could be obtained through the first cyclization reaction from **S2** and 4-*N*-Boc-aminophenol, followed by the second cyclization reaction to obtain isatin **S5**. Plasiatine and its isomers are expected to be obtained from **S5** through an addition reaction.

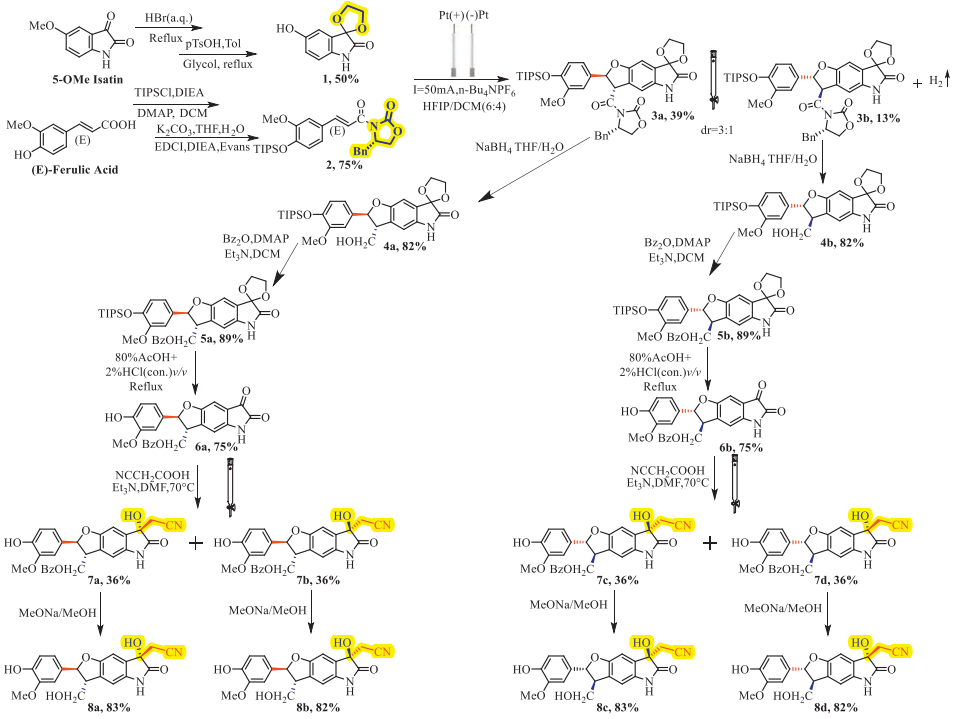
We first explored the cyclization reaction since the construction of dihydrofuran moiety was important in both routes. 4-*N*-Boc-aminophenol and ethyl ferulate were successfully coupled to construct the dihydrofuran moiety utilizing a radical α-addition involved electro-oxidative [3 + 2] annulation [35]. Regrettably, subsequent cyclization to form isatin moiety was unsuccessful. Moreover, **S2** failed to cyclize with most 5–hydroxy-indole derivatives (**S3a-c**, Scheme S2 in Supporting information).

Nonetheless, **S2** could be coupled with 5–hydroxy-2-oxindole to obtain **S3d**. Although subsequent oxidation of **S3d** to form isatin was also unsuccessful, this result suggested that the electron-withdrawing group at indole C3 was detrimental to the annulation reaction. Consequently, we hypothesized that introduction of ketal at 5-hydroxyisatin C3 position could reduce the electron-withdrawing effect and facilitate the electro-oxidative [3 + 2] annulation reaction. Our hypothesis was validated when **S3e** was successfully synthesized from compound **1** and ethyl ferulate. To facilitate separation of the enantiomer, ferulic acid was orthogonally protected and Evans chiral auxiliary was introduced at the carboxyl group, yielding compound **2**. After optimization of the reaction conditions (Table S1 in Supporting information) **3a** and **3b** were obtained in a 3:1 diastereomeric ratio with yields of 39% and 13%, respectively. The Evans auxiliary was then reduced by $NaBH_4$ to yield **4a** and **4b** with an 82% yield, followed by benzoylation of the primary alcohol to obtain **5a** and **5b** in 89% yield, which modulated the molecular polarity to facilitate separation of the subsequent epimers. The deprotection procedure of ketal and silyl was carried out under reflux in an aqueous solution of 80% CH_3COOH and 2% concentrated HCl to obtain **6a** and **6b** in 75% yield. Subsequently, **7a**, **7b** and **7c**, **7d** were obtained by addition of **6a** and **6b** with cyanoacetic acid, which could be separated by column chromatography. Finally, plasiatine and its isomers (**8a**–**8d**) were obtained through a standard deprotection procedure in MeONa/MeOH with 82% yield. In summary, plasiatine and its isomers were synthesized for the first time through a radical α-addition involved electro-oxidative [3 + 2] annulation, followed by twice convenient separations of diastereoisomers with column chromatography in 8 linear steps with overall yields of 3.2% for **8a**, 3.2% for **8b**, 1.1% for **8c** and 1.1% for **8d** (Scheme 1).

Upon completion of the total synthesis, we proceeded with the structural identification of the synthesized compounds, which provided definitive evidence that isomer **8b** is indeed the natural product plasiatine (Figs. S2–S7 in Supporting information).

To explore the influence of chiral centers on the biological activity, the enzymatic activities of all isomers were measured using 6,8-difluoro-4-methylumbelliferyl phosphate (DiFMUP) as a substrate [36]. The result revealed that **8a** had a stronger activation effect than plasiatine in the SHP2-PTP domain. In contrast, isomers **8c** and **8d** did not show any significant activating or inhibiting activity (Fig. 1A). These findings suggested that the stereochemistry of the dihydrofuran ring was crucial for the SHP2-activating effect. Since the SHP2 protein is known to play a significant role in the mitogen-activated protein kinase (MAPK)/extracellular signal-regulated kinase (ERK) pathway [37], we investigated the effects of **8a** and **8b** on this pathway in the MV4–11 and DU145 cell lines, with SHP099 (a potent SHP2 inhibitor) [38,39] and lovastatin (a moderate activator) [17] as controls. Western blot (WB) revealed that both **8a** and **8b** induced the phosphorylation of ERK 1/2 in a dose-dependent manner across both cell lines (Figs. 1B and C). However, **8a** was significantly more potent than **8b** and was observed to stimulate the phosphorylation of ERK 1/2 in DU145 cells in a time-dependent manner (Fig. 1D). To identify whether the target of **8a** is SHP2, SW480 cells were transfected with siRNA to downregulate SHP2 expression level. Subsequently, both the control and SHP2 knockdown groups were treated with 50 and 100 μmol/L of **8a** for 24 h, respectively. WB results indicated that upon SHP2 knockdown with siRNA, the ability of **8a** to activate the phosphorylation of ERK was significantly diminished. In contrast, **8a** maintained its capacity to activate ERK 1/2 phosphorylation in the control group (Fig. 1E). To further validate the target of **8a**, a cellular thermal shift assay (CETSA) was performed in MV4–11 cells. The CETSA result demonstrated that the thermal stability of SHP2 in MV4–11 cells was significantly increased in the presence of **8a** compared with the control group (DMSO). These findings provided compelling evidences that **8a** directly interacted with SHP2 (Figs. 1F and G).

Molecular docking was conducted to elucidate the difference of binding modes between **8a** and **8b**. As depicted in the Figs. S9B and D (Supporting information), both the **8a** and **8b** indole moieties were well positioned in the catalytic pocket. In the binding mode of **8b** and catalytic pocket (Fig. S9A in Supporting information), the oxoindoline carbonyl established two hydrogen bonds with Arg465 (2.9 and 3.5 Å), the tertiary hydroxyl group engaged in two hydrogen bonds with Gln506 (2.9 Å) and Gln510 (2.9 Å), and the acetonitrile group formed hydrogen bond with Gly464 (3.1 Å). The hydroxymethyl group, positioned at the edge of the PTP pocket (E loop), interacted with residue Lys366 (3.2 Å) through hydrogen bond interaction. Additionally, there was a π-π stacking interaction between the phenyl ring and Tyr279 (5.3 Å). **8a** also bound to the catalytic pocket through a network of hydrogen bond interactions (Fig. S9C in Supporting information). Specifically, the oxoindoline carbonyl formed hydrogen bond with Arg464 (3.2 and 3.4 Å), the tertiary hydroxyl group engaged in two hydrogen bonds with Gln506 (2.6 Å) and Gln510 (3.2 Å), and the acetonitrile group formed hydrogen bonds with Lys366 (3.4 Å). Although hydrogen bond interaction network established between the indole ring and the PTP pocket appeared to be somewhat weakened, the cation-π interaction was established between the indole ring and Lys366 (3.7 Å), as well as between the phenyl ring and Lys364 (3.4 Å). The cation-π interaction plays a significant role in molecular recognition and can greatly influence the binding affinity between a lig-



Scheme 1. Total synthesis of plasiatine and its isomers.

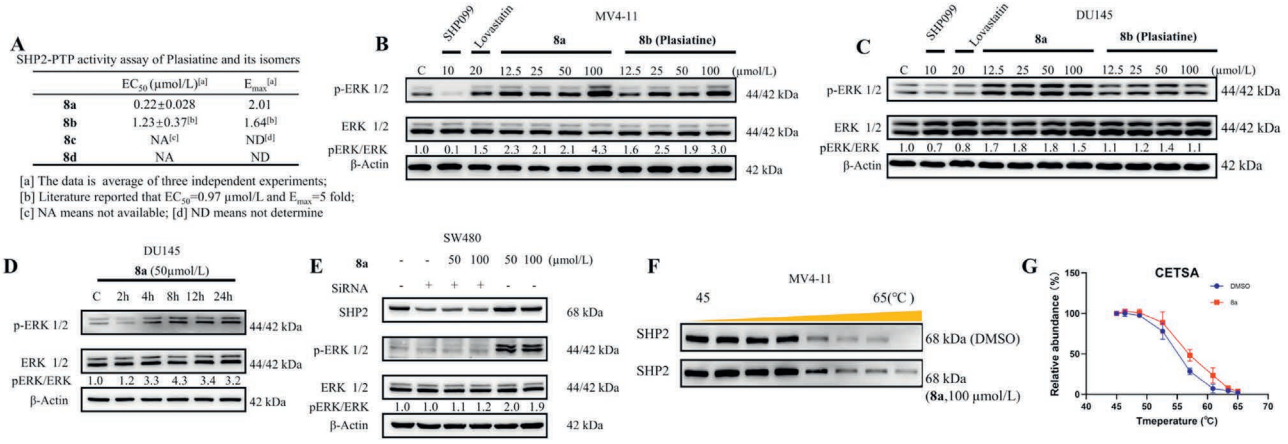


Fig. 1. Evaluation of SHP2 activity, cell activity of plasiatine and its isomers. (A) SHP2 activity assay of **8a**–**8d** in SHP2 PTP domain. (B, C) WB of MV-4–11 and DU145 cells incubated with **8a** and **8b** for 24 h. (D) Time-dependent activating ERK effect of **8a** in DU145 cells. (E) SHP2 knockdown with siRNA in SW480 cells. (F, G) CETSA between **8a** and SHP2 in MV4–11 cells. The SHP2 relative abundance was measured by Image J, and the data were shown as means ± SEM.

and and its binding pocket [40]. Furthermore, a new hydrogen interaction was also formed between the hydroxymethyl group and Lys364 (3.1 Å). The interaction between **8a** and Lys364 allowed it to conform more closely to the E Loop, which could potentially activate SHP2 and improve its phosphatase activity as previously reported [16]. However, **8a** lost the π-π stacking interaction with Tyr279 (pTyr Loop), and whether the introduction of interaction with Tyr279 could further enhance the activation effect is worthy of further investigation.

As indicated in Table S4 and Fig. S10 (Supporting information), we explored the impact of various substituents introduced at the indole ring C3 position, considering the hydrogen bond interaction with the PTP catalytic pocket. However, we found that these modifications did not lead to significant enhancement in potency. The replacement of ethyl cyanide with allyl cyanide, hydroxymethyl and hydroxyethyl groups led to varying degrees of activity loss (**A1**–**A4**). The introduction of acetylmethyl diminished the potency (**A5**, **A6**), and while the benzoylmethyl substituent **A7** maintained activity, its epimer **A8** showed a decrease in activity with $EC_{50} = 3.54$ μmol/L. Similarly, the introduction of a thienylcarbonyl group attenuated the activity (**A9**), and the activity of **A10** was even completely lost. An allyl group substitution was also not conducive to improve the potency (**A11**, **A12**). The introduction of a carbethoxy group and α-picoline led to deactivation (**A13**–**A15**). The tertiary hydroxy was proved essential for maintaining activity (**A16**). The difluoro substituent in **A17** did not demonstrate significant activity improvement either.

Enzymatic activity assays (Table S4) indicated that compound **B1** exhibited a moderate activation effect with $EC_{50} = 0.68$ μmol/L and $E_{max} = 1.54$-fold. Given that some indole-based SHP2 orthosteric inhibitors had been reported [41], we sought to explore whether the introduction of double bond substituents at the indole C-3 position could maintain the activation effect [41]. However, we found that the introduction of such substituents led to a loss of

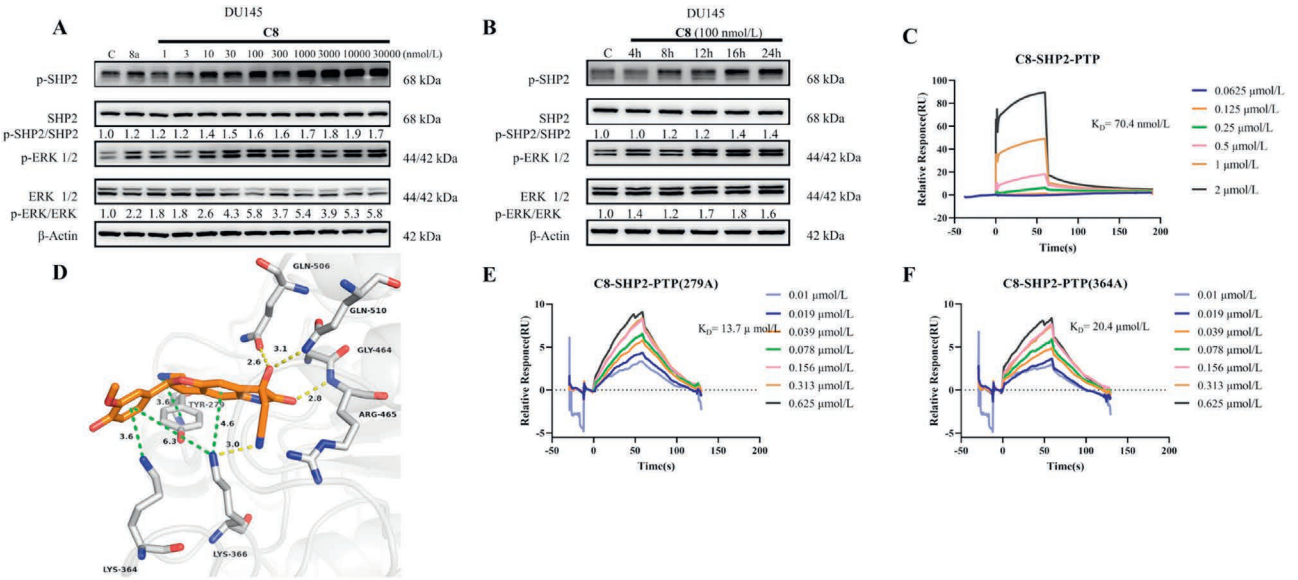


Fig. 2. Characterization of the target of **C8**. (A, B) Concentration and time-dependent activating SHP2 of **C8** in DU145 cells. (C) SPR of **C8** and SHP2-PTP. (D) Molecular docking of **C8** in SHP2 PTP domain (PDB ID: 4PVG). (E) SPR of **C8** and SHP2-PTP (279A). (F) SPR of **C8** and SHP2-PTP (364A).

activity and even an inhibitory effect (**B2**–**B9**). This result suggests that while the indole scaffold is a promising starting point for the development of SHP2 modulators, the specific substitution pattern is crucial for maintaining the desired activity.

The hydroxymethyl group, located at the edge of the PTP pocket (E loop), is another potential modification site. Replacing the hydroxyl group yielded compounds **C1**–**C9**. The introduction of ester and amide groups resulted in a loss of activity (**C1**–**C3**), but deoxofluorination of the hydroxyl group increased the potency with $EC_{50} = 0.14$ μmol/L (**C5**). Subsequently, replacing the hydroxyl group with an amino group surprisingly demonstrated a remarkable increase in activity, with $EC_{50} = 0.11$ μmol/L and $E_{max} = 3.75$-fold (**C8**). **C9**, the 7-epimer of **C8**, showed activity comparable to compound **8a**. **C6** and **C7**, as the precursor of **C8** and **C9** respectively, did not show significant increase in activity. X-ray crystallography of **C9** derivative **C9a** revealed that the quaternary chiral center at the indole C-3 was *R*-configuration, which was consistent with **8b**, indicating that the indole ring C-3 of **C8** mantained a *S*-configuration, consistent with **8a**.

Upon observing that most SHP2 activators possessed aliphatic side chains, we chose to introduce a series of alkyl substituents on the phenolic hydroxyl group to assess their effects on activity (**D1**–**D10**). However, our attempts did not produce a significant increase in activity. To further investigate the influence of the amino group of **C8** on the biological activity, we undertook a series of modifications at the amino group to yield **C8a**–**C8e**. Acetylation resulted in an inhibitory effect (**C8a**), while mesylation, thioureido substitution, guanidine substitution and methylation all led to moderate even sharp decrease in activity (**C8b**–**C8e**), indicating that the amino group was the most suitable substituent.

The effect of **C8** on the SHP2 and MAPK/ERK signaling pathway was investigated in DU145 cells. As depicted in Fig. 2A, **C8** demonstrated the ability to increase the phosphorylation levels of SHP2 and ERK1/2 in a concentration-dependent manner. Remarkably, **C8** exhibited a potent activating effect with a more pronounced activation of SHP2 and ERK at a concentration as low as 30 nmol/L compared to **8a** at 30 μmol/L. Additionally, **C8** triggered a time-dependent activation of SHP2 and ERK at 100 nmol/L. The activation of SHP2 became evident 8 h post-treatment, the activation of ERK peaked at 12 h, and this effect persisted up to 24 h post-treatment (Fig. 2B).

Surface plasmon resonance (SPR) experiments were conducted to reveal the robust affinity between **C8** and the SHP2 PTP domain with $K_d = 70.4$ nmol/L (Fig. 2C). Molecular docking was performed to elucidate the binding mode of **C8** in the catalytic pocket and to rationalize its potent activation effect. As depicted in Fig. 2D, **C8** was found to be situated in the PTP domain, analogous to the positioning of **8a**. The indole moiety of **C8** engaged in hydrogen bond interactions with Lys366 (3.0 Å), Gln506 (2.6 Å), Gln510 (3.1 Å), and Arg465 (2.8 Å), which appeared to be less robust compared to **8a**. Concurrently, **C8** retained the cationic-π interaction with Lys364 (3.6 Å) and Lys366 (4.6 Å). Surprisingly, a cationic-π interaction was formed between the -NH_2 and Tyr279 (3.6 Å), alongside a weaker cationic-π interaction between the phenol ring and Lys366 (6.3 Å). Mutation of Y279C had been implicated in abnormal SHP2 activation and was associated with developmental diseases like Noonan syndrome [42]. Therefore, the interaction with Tyr279 might facilitate the activation of SHP2 by competing pTyr ligands [43]. Furthermore, Tyr279 and Lys364 were mutated to alanine (Ala). SPR analysis demonstrated that the affinity of **C8** to SHP2-PTP-Y279A ($K_d = 13.7$ μmol/L) and SHP2-PTP-K364A ($K_d = 20.4$ μmol/L) was sharply decreased compared with SHP2 PTP wild type (Figs. 2E&F). Although it seemed counterintuitive to enhance SHP2 activity by occupying the active site, the transition from plasiatine to **C8** showed a trend where binding to the catalytic core weakened while interactions with the surrounding loops intensified. This observation implied that **C8** might induce a conformational change in the active pocket of PTP, thereby enhancing its catalytic activity.

The selectivity of compounds **8a**, **8b** and **C8** were investigated on SHP2, SHP1-PTP and PTP1B utilizing the DiFMUP phosphate fluorescence assay (Figs. S11 and S12 in Supporting information). To investigate the anti-atherosclerotic effect of **C8**, an ox-LDL-induced THP-1 cell model was established. After differentiation of THP-1 cells into M0 macrophages induced by PMA (25 ng/mL, 48 h), the cells were treated with various concentrations of **C8**, with Lovastatin serving as a control, and co-incubated with 50 μg/mL of ox-LDL for 48 h. WB analysis demonstrated that **C8** could elevate phosphorylation level of SHP2 and expression of PPARγ in a concentration-dependent manner consistent with the report (Fig. 3A) [32]. To explore the *in vivo* anti-atherosclerotic effects of **C8**, an atherosclerosis model was established using $ApoE^{-/-}$ mice. All

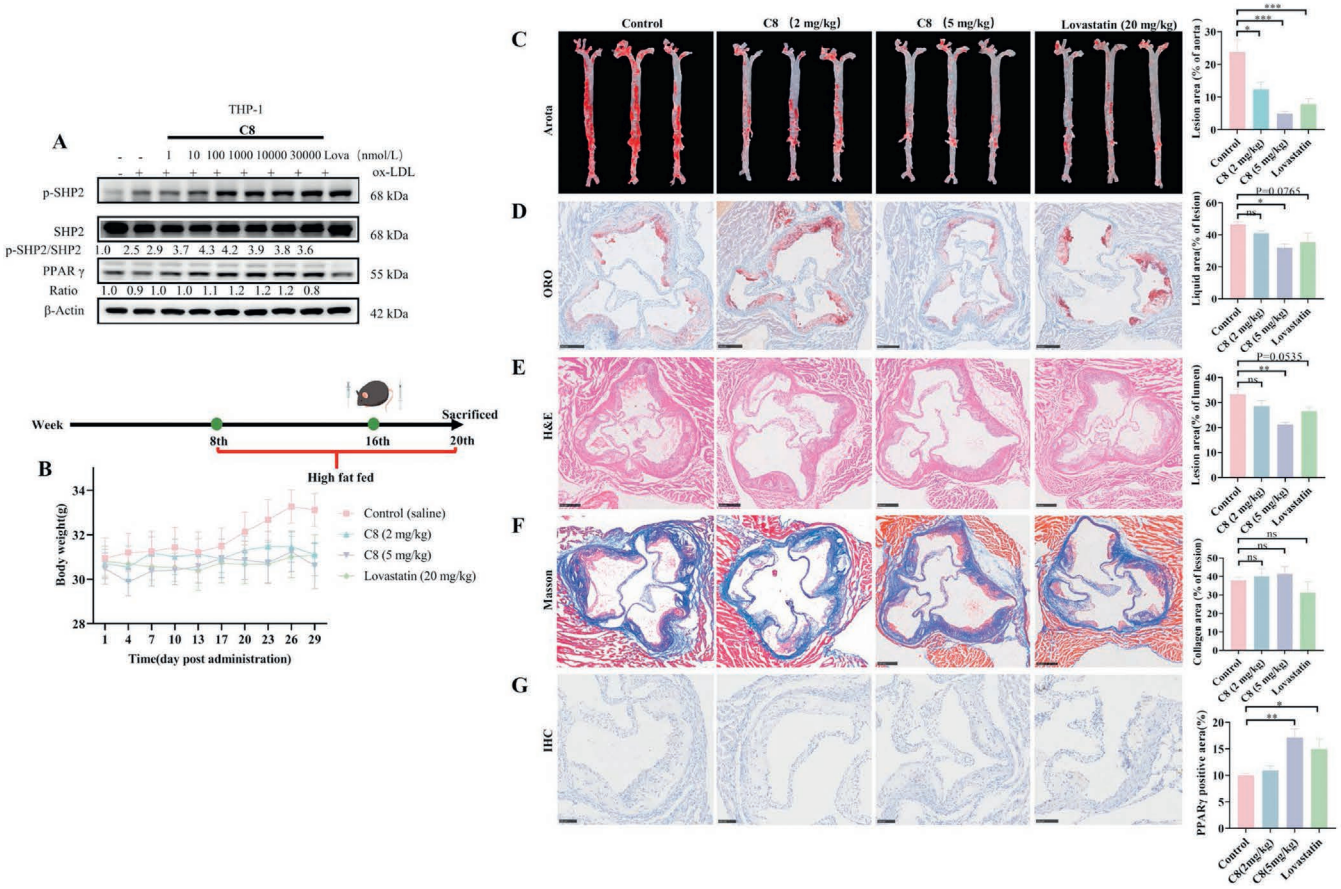


Fig. 3. Evaluation of the anti-atherosclerosis effect of **C8**. (A) THP-1 cell model induced by ox-LDL. (B) Time line of treatment for high fat fed (HIF) ApoE$^{-/-}$ mice. Body weights of mice were measured every three days post administration ($n = 7$–9). (C) Representative images of aortas stained with ORO ($n = 5$). (D) Plaque deposition in the aortic root with ORO staining ($n = 4$). Scale bar: 250 μm. (E) Lesion in the aortic root with H&E staining ($n = 4$). Scale bar: 250 μm. (F) Lesion in the aortic root with Masson's trichrome stain ($n = 4$). Scale bar: 100 or 250 μm. (G) PPARγ staining for aortic roots with immunohistochemistry ($n = 3$). Scale bar: 50 μm. Data were shown as means ± SEM. The statistical significances were calculated *via* one-way ANOVA. $^{*}P < 0.05$, $^{**}P < 0.01$, $^{***}P < 0.001$. ns, non-significant; IHC, immunohistochemical.

animal experiments have been granted approval by the Institutional Animal Care and Use Committee (IACUC) of Peking University Health Science Center (No. LA2017039) and strictly abide by the ethical guidelines established by Peking University Health Science Center. The mice were randomly assigned to control (saline), low-dose (**C8**, 2 mg/kg, iv), high-dose (**C8**, 5 mg/kg, iv), and positive drug groups (lovastatin, 20 mg/kg, po). All mice were fed with a Western diet for 8 weeks before treatment with **C8** or lovastatin (Fig. 3B). Body weight was monitored every three days post administration. From day 20 post-administration, a noticeable increase in body weight was observed in the control group, while the treatment group remained relatively stable. After dissection, the whole aortas were stained with Oil Red O (ORO), and the dosed groups were comparable to the positive drug groups. Analysis of the plaque deposition area in the aortic root revealed a reduction in plaque accumulation in the high-dose group compared to the control group (Figs. 3C and D). The lesion areas were distinguishably decreased in both high-dose group and positive group through hematoxylin and eosin staining (H&E) staining (Fig. 3E). Masson's trichrome staining indicated no significant difference in collagen content (Fig. 3F). Peritoneal macrophages (PMs) were isolated for enzyme-linked immunosorbent assay (ELISA) assay (Fig. S13A), which revealed a significant increase in the levels of anti-inflammatory factors (mannose receptor C-type 1 (MRC1), resistin-like molecule alpha (Fizz1) and arginase 1 (ARG1)) in the supernatant of PMs, accompanied by a decrease in pro-inflammatory factors (tumor necrosis factor alpha (TNFα), interleukin-1 beta (IL-1β)). WB analysis demonstrated that PMs of the high-dose group exhibited a high level of SHP2 activation with the highest expression level of PPARγ (Fig. S13B). The increased expression of PPARγ in the aortic root lesion area due to SHP2 activation was also verified by immunohistochemical analysis (Fig. 3G).

In conclusion, we report the first total synthesis of plasiatine and its three isomers, achieved through an electro-oxidative [3 + 2] annulation reaction, with two convenient separations of diastereoisomers by chromatography, all within 8 linear steps. Preliminary activity assay revealed that **8a** (the 7-epimer of plasiatine) exhibited superior activation effect compared to the natural product plasiatine. Further exploration of the structure-activity relationship led to the identification of compound **C8**, which demonstrated a potent activation effect at the cellular level with an $EC_{50} = 0.11$ μmol/L and $E_{max} = 3.75$-fold. SPR experiments indicated that **C8** had a strong affinity for the PTP domain with a $K_d = 70.4$ nmol/L and molecular docking and protein site-directed mutagenesis revealed that Tyr279 and Lys364 play essential roles. *In vitro* THP-1 cell model induced by ox-LDL showed that activated SHP2 by **C8** could enhance the expression of PPARγ in a concentration-dependent manner. In the ApoE$^{-/-}$ atherosclerosis mice model, **C8** significantly reduced atherosclerotic plaques, decreased lesion area at a daily dose of 5 mg/kg. ELISA assay results indicated that **C8** could markedly elevate the levels of anti-inflammatory factors while reducing pro-inflammatory factors in the supernatant of PMs. Collectively, our research demonstrated that **C8** was a highly potent SHP2 activator, providing a powerful

tool molecule for the study of the biological function of SHP2 and warranted further investigation to elucidate the specific activation mechanism.

CRediT authorship contribution statement

Xuyang Ding: Writing – review & editing, Writing – original draft, Visualization, Validation, Methodology, Investigation, Formal analysis, Data curation, Conceptualization. **Tongtong Geng:** Validation, Investigation. **Yongxia Li:** Validation. **Pengming Pan:** Methodology, Data curation. **Zhongtang Li:** Conceptualization. **Zhongjun Li:** Supervision, Project administration, Funding acquisition, Conceptualization. **Xiangbao Meng:** Writing – review & editing, Validation, Supervision, Resources, Project administration, Methodology, Investigation, Funding acquisition, Conceptualization.

Declaration of competing interest

The authors declare that they have no known competing financial interests or personal relationships that could have appeared to influence the work reported in this paper.

Acknowledgments

We gratefully acknowledge Beijing Natural Science Foundation (No. 7232254) for generous financial support. Special thanks to our colleague Dr. Ao Sun for the help of experimental discussion.

Supplementary materials

Supplementary material associated with this article can be found, in the online version, at doi:10.1016/j.cclet.2025.112140.

References

[1] P. Hof, S. Pluskey, S. Dhe-Paganon, et al., Cell 92 (1998) 441–450.
[2] Q. Nian, J. Zeng, L. He, et al., Chin. Chem. Lett. 32 (2021) 1645–1652.
[3] Y.H. Song, M. Zhao, H.Q. Zhang, B. Yu, Pharmacol. Ther. 230 (2022) 107966.
[4] M. Dance, A. Montagner, J.P. Salles, et al., Cell. Signal. 20 (2008) 453–459.
[5] S.Q. Zhang, W.G. Tsiaras, T. Araki, et al., Mol. Cell. Biol. 22 (2002) 4062–4072.
[6] C.J. Wu, D.M. O'Rourke, G.S. Feng, et al., Oncogene 20 (2001) 6018–6025.
[7] D. Xu, C.K. Qu, Front. Biosci. 13 (2008) 4925–4932.
[8] M.X. Zhao, W.J. Guo, Y.Y. Wu, et al., Acta Pharm. Sin. B 9 (2019) 304–315.
[9] T. Yokosuka, M. Takamatsu, W. Kobayashi-Imanishi, et al., J. Exp. Med. 209 (2012) 1201–1217.
[10] Y. Liu, J. Liang, M. Zheng, et al., Chin. Chem. Lett. 36 (2025) 110317.
[11] P.S.Y. Chong, J.B. Zhou, J.S.L. Lim, et al., Cancer Res. 79 (2019) 4679–4688.
[12] P.F. Cai, W.J. Guo, H.Q. Yuan, et al., Biomed. Pharmacother. 68 (2014) 285–290.
[13] J. Pan, L.S. Zhou, C.Y. Zhang, et al., Signal Transduct. Target. Ther. 7 (2022) 24.
[14] Y. Liu, X.H. Yang, Y.L. Wang, et al., Eur. J. Med. Chem. 214 (2021) 113264–113280.
[15] Y. Jin, Y.J. Yoon, Y.J. Jeon, et al., Biochem. Pharmacol. 142 (2017) 46–57.
[16] J.B. Hu, W. Liu, Y. Zou, et al., Acta Pharm. Sin. B 14 (2024) 2598–2612.
[17] W. Liu, M.J. Wang, L.H. Shen, et al., Signal Transduct. Target. Ther. 6 (2021) 3.
[18] Z.H. Gao, Y.M. Shi, Z. Qiang, et al., Sci. Rep. 6 (2016) 9.
[19] Y.Y. Bu, T. Shi, M.H. Meng, et al., Bioorg. Med. Chem. Lett. 21 (2011) 874–878.
[20] Y.J. Lee, H. Song, Y.J. Yoon, et al., Biochem. Pharmacol. 175 (2020) 12.
[21] X.Q. Wang, A.H. Zhang, J. Gao, et al., J. Invest. Dermatol. 134 (2014) 2737–2746.
[22] X.X. Wu, W.J. Guo, L.M. Wu, et al., J. Immunol. 189 (2012) 3497–3507.
[23] P.G. Song, Z. Fang, H.Y. Wang, et al., Lancet Glob. Health 8 (2020) E721–E729.
[24] L.I. Susser, K.J. Rayner, J. Clin. Invest. 132 (2022) 10.
[25] A.R. Tall, D.G. Thomas, A.G. Gonzalez-Cabodevilla, I.J. Goldberg, J. Clin. Invest. 132 (2022) 11.
[26] A. Trzeciak, Y.T. Wang, J.S.A. Perry, Cell Metab. 33 (2021) 2126–2141.
[27] X. Chai, H.L. Ngan, Y. Song, et al., Chin. Chem. Lett. 36 (2025) 110671.
[28] M. Bäck, A. Yurdagul, I. Tabas, et al., Nat. Rev. Cardiol. 16 (2019) 389–406.
[29] S.E. Engelen, A.J.B. Robinson, Y.X. Zurke, C. Monaco, Nat. Rev. Cardiol. 19 (2022) 522–542.
[30] O. Soehnlein, P. Libby, Nat. Rev. Drug Discov. 20 (2021) 589–610.
[31] P. Kong, Z.Y. Cui, X.F. Huang, et al., Signal Transduct. Target. Ther. 7 (2022) 24.
[32] C.X. Wu, P.Y. Zheng, L. Ma, et al., Arterioscler. Thromb. Vasc. Biol. 44 (2024) 202–217.
[33] T. Deng, H.J. Wang, C. Cai, Eur. J. Org. Chem. 2014 (2014) 7259–7264.
[34] V.P.R. Gajulapalli, P. Vinayagam, V. Kesavan, Org. Biomol. Chem. 12 (2014) 4186–4191.
[35] Q. Zhao, J.K. Jin, J. Wang, et al., Chem. Sci. 11 (2020) 3909–3913.
[36] K.R. Gee, W.C. Sun, M.K. Bhalgat, et al., Anal. Biochem. 273 (1999) 41–48.
[37] S. Bunda, K. Burrell, P. Heir, et al., Nat. Commun. 6 (2015) 12.
[38] Y.N.P. Chen, M.J. LaMarche, H.M. Chan, et al., Nature 535 (2016) 148–152.
[39] J.G. Fortanet, C.H.T. Chen, Y.N.P. Chen, et al., J. Med. Chem. 59 (2016) 7773–7782.
[40] K. Kumar, S.M. Woo, T. Siu, et al., Chem. Sci. 9 (2018) 2655–2665.
[41] H.R. Lawrence, R. Pireddu, L.W. Chen, et al., J. Med. Chem. 51 (2008) 4948–4956.
[42] M. Tartaglia, E.L. Mehler, R. Goldberg, et al., Nature Genet. 29 (2001) 465–468.
[43] Z.H. Yu, R.Y. Zhang, C.D. Walls, et al., Biochemistry 53 (2014) 4136–4151.